Int. J. Solids Structures, 1965, Vol. 1, pp. 319 to 341. Pergamon Press Ltd. Printed in Great Britain

THE DYNAMIC STABILITY OF RAILWAY VEHICLE WHEELSETS AND BOGIES HAVING PROFILED WHEELS

A. H. WICKENS

British Rail Research Department, Derby

Abstract—The dynamic instability of railway vehicle bogies and wheelsets is caused by the combined action of the conicity of the wheels and the creep forces acting between the wheels and rails. In this paper, the instability is investigated in the important case where the wheels are profiled rather than purely conical. Equations of motion are formulated and stability criteria obtained which indicate the effect of varying the various parameters of the system. The nature of the motion at the critical speed is investigated and the mode of energy conversion between the forward motion of the vehicle and the lateral motion of the bogie or wheelset is explained.

NOTATION

$2a$	length of contact area in direction of rolling
a_1, a_2	relative amplitudes of generalised coordinates ϕ_1 and ϕ_2
$2b$	length of contact area transverse to direction of rolling
C	moment of inertia in yaw of wheelset
d	length, defined in Fig. 1
d_1, d_2	suspension viscous damping coefficients in longitudinal and lateral directions
f, f'	longitudinal and lateral creep coefficients
F	dissipation function
G	modulus of rigidity
j	$= C/ml^2$
$\bar{j}$	moment of inertia of bogie divided by ml^2
k_1, k_2	suspension elastic stiffness coefficients in longitudinal and lateral directions
l	length, defined in Fig. 1
m	mass of wheelset
M	tractive torque
N, N'	normal reactions at contact points
p_i	coefficients in characteristic equation
P	tractive force
q_1	lateral displacement of wheelset or bogie
q_2	yaw of wheelset or bogie
Q_1	lateral force exerted by rails on wheelset
Q_2	yawing moment exerted by rails on wheelset
r_0	wheel tread circle radius, wheelset in central position
r, r'	radii of tread circles, wheelset displaced laterally
R	radius of curvature of wheel tread
R'	radius of curvature of rail head
s	$= \frac{l}{V_0}\frac{\mathrm{d}}{\mathrm{d}t}$
t	time
T	kinetic energy
v	$= V/V_0$
v_0, v_c	non-dimensional critical speeds
V	forward speed of vehicle; potential energy
V_0	reference speed
W	axle-load

α	$= \lambda l/r_0$
β	length, defined in Fig. 1
γ, γ'	longitudinal and lateral creepages
γ	mass of bogie divided by mass of wheelset
δ, δ'	angle between contact plane and horizontal at contact points
δ_0	angle between contact plane and horizontal, wheelset in central position
ε	defined by equation (3)
$\varepsilon_1, \varepsilon_2, \bar{\varepsilon}_2$	non-dimensional stiffness coefficients
ζ_1, ζ_2	non-dimensional damping coefficients
λ	effective conicity
λ_i	$= \eta_i + i\nu_i$, root of characteristic equation
θ	phase angle
μ, μ'	non-dimensional creep coefficients
ν	$= \omega l/V_0$
ϕ_1	$= q_1/l$
ϕ_2	$= q_2$
Φ, ψ_1	functions of (a/b) involved in calculation of creep coefficients
ω	circular frequency
Ω	$= Vl/V_0r_0$

INTRODUCTION

AT CERTAIN forward speeds, some railway vehicles experience sustained oscillations in the lateral plane. These oscillations arise because of the dynamic instability of these vehicles caused by interaction between the conicity of the wheels, the forces acting between the wheels and the rails and the action of the suspension. Railway vehicles were originally provided with coned wheels in order to obtain a measure of static stability, but as wheel treads rapidly wear with use, wheels which commence life with conical treads come to possess concave treads which possess curvature in the transverse direction. The behaviour of a vehicle with profiled wheels of this type is significantly different from that of a vehicle with coned wheels, and this paper presents a general theory of the stability of the small oscillations of elastically restrained wheelsets (a wheelset consisting of two wheels mounted on a rigid, common axle) and bogies having profiled wheels.

The system considered consists of a single wheelset or bogie (Fig. 1) connected by means of an elastic suspension to a vehicle body which is assumed to move forward at constant velocity with negligible lateral motion. The suspension possesses flexibility in the longitudinal and lateral directions. The bogie consists of two wheelsets mounted, without lateral or longitudinal flexibility, in a rigid frame. The neglect of the lateral motions of the vehicle body can be justified in general terms on the basis that the body has a much greater mass than a wheelset or bogie and that the instability discussed here occurs at frequencies which are much higher than the natural frequencies of the body oscillating on the suspension. A more specific justification can be given by considering the stability of a complete vehicle with appropriate body freedoms; this will be done in a sequel to this paper.

It is well known that an elastic structure which is subject to non-conservative forces may become dynamically unstable under certain conditions of loading. Apart from the instabilities of other wheeled vehicles, such as shimmy of automobiles, examples of elastic systems of this kind are provided by structures loaded by aerodynamic or hydrodynamic forces, rotating shafts and servo-mechanisms with structural feedback; the nature of the instabilities of systems of this type has been discussed by Bolotin [1]. In the system discussed here the non-conservative forces arise from the phenomenon of creep. When elastic bodies roll together, contact takes place over an area which can be determined by the theory of Hertz. It has been found that a tangential force transmitted across the contact area will cause a relative velocity, or creep, of one surface relative to the other. Provided that the tangential force is less than about one third of that necessary to produce sliding of one body over the other, the creep velocity is proportional to the tangential force. Creep arises because, in the contact area, there is a region of adhesion and a region of slipping in which the tangential traction is equal to the limiting friction. The creep velocity is consistent with the difference in the elastic strains between the two bodies in the region of adhesion. As the magnitude of the tangential force increases, the region of slipping occupies a larger proportion of the contact area, until sliding occurs as the tangential force equals the limiting friction. For small values of the creep velocity, slipping is confined to the trailing edge of the contact area and the phenomenon is independent of the coefficient of friction, being governed only by the elastic strain distribution in the vicinity of the contact area.

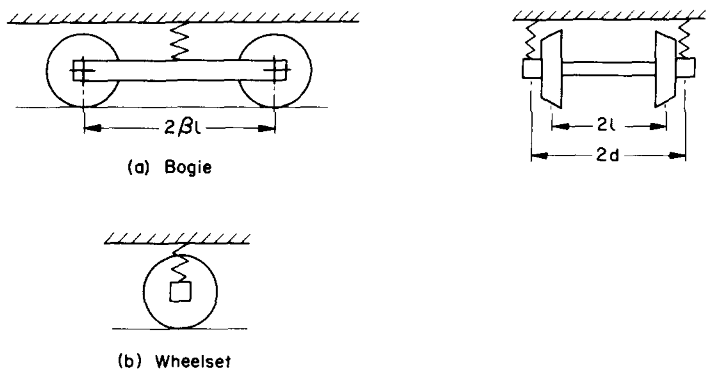

FIG. 1. Elastically restrained wheelset and bogie.

Carter [2] recognized the importance of the phenomenon of creep in the lateral dynamics of railway vehicles, and considered the stability of various configurations of locomotives [3], indicating the existence of critical speeds separating regions of stable and unstable motions. Previously, a theoretical analysis of the kinematic oscillation of a slowly rolling wheelset with coned wheels had been given by Klingel [4]. The stability of locomotives was also considered by Rocard [5], and a discussion of stability using the concept of energy balance was given by Cain [6]. Up to this time, only conical wheels had been considered but Davies [7] and Davies and Cook [8] investigated the motions of wheelsets experimentally and theoretically and indicated the importance of the wheel and rail profiles. The effect of wear of the wheel tread on the kinematic oscillation was discussed by Heumann [9]. For profiled wheels, the lateral component of the change in the normal reactions between wheel and rail as the wheelset is displaced is proportional to the lateral displacement. This effect was included in studies made by de Possel and Beautefoy [10] and by Müller [11]. The stability of a rigid trolley with coned wheels has been considered by Brann [12] and the stability of a complete vehicle with coned wheels by Matsudeira [13]. Certain non-linear aspects of the lateral dynamics of railway vehicles have been considered by de Pater and Katz [14].

EQUATIONS OF MOTION OF THE ELASTICALLY RESTRAINED WHEELSET

A wheelset which is moving along the track at constant speed has two degrees of freedom, and appropriate generalized coordinates are q_1, the lateral displacement of the centre of mass of the wheelset, and q_2 the angle of yaw of the wheelset. Local deflections of the wheelsets and rails at the points of contact will be neglected in the formulation of the equations of motions, which are

$$\begin{aligned} m\ddot{q}_1 + 2d_2\dot{q}_1 + 2k_2 q_1 &= Q_1, \\ C\ddot{q}_2 + 2d^2 d_1 \dot{q}_2 + 2d^2 k_1 q_2 &= Q_2, \end{aligned} \tag{1}$$

where the generalized forces Q_1 and Q_2 represent the forces acting between the wheels and the rails, m is the mass of the wheelset, C the moment of inertia in yaw, k_1 and k_2 represent the suspension stiffnesses in the longitudinal and lateral directions and d_1 and d_2 represent the corresponding suspension dampings.

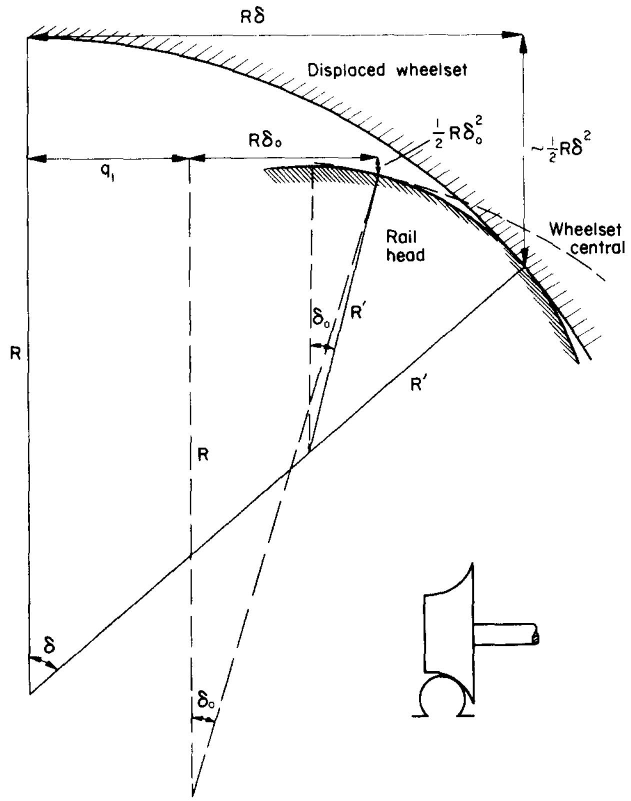

FIG. 2. Geometry of wheel and rail contact.

It will be assumed throughout the analysis that the angle made by the contact plane with the horizontal, δ_0, at each of the contact points when the wheelset is in the centre position is a small quantity of the same order as the generalized displacements, so that for the small displacements considered here, products of δ_0 with q_1 or q_2 and their derivatives are negligible. The angle of roll of the wheelset as it is displaced laterally is then a second order quantity, and gyroscopic forces may be omitted from equations (1).

When the wheels are in the central position on the track, the tread circles of both wheels of the wheelset have the same radius r_0. When the wheelset is displaced laterally, contact occurs at new points (Fig. 2) and the angles made by the contact planes at these points are denoted by δ and δ' respectively, and the radii of the tread circles become r and r'. If R is the radius of curvature of the wheel tread and R' is the radius of curvature of the rail head, then for small displacements reference to Fig. 2 shows that

$$q_1 + R\delta_0 - R'\delta_0 + R'\delta = R\delta,$$

or

$$\delta - \delta_0 = q_1/(R-R'),$$

so that

$$\delta = \delta_0 + \frac{\varepsilon q_1}{l}, \tag{2a}$$

where

$$\varepsilon = l/(R-R'). \tag{3}$$

Similarly

$$\delta' = \delta_0 - \frac{\varepsilon q_1}{l}. \tag{2b}$$

Also from Fig. 2 it follows that

$$\begin{aligned} r - r_0 &= \frac{R}{2}(\delta^2 - \delta_0^2) \\ &= \frac{R}{2}(\delta-\delta_0)(\delta+\delta_0) \\ &= R(\delta-\delta_0)\delta_0 \qquad \text{approximately}, \\ &= R\varepsilon\delta_0 q_1/l. \end{aligned}$$

Thus

$$r = r_0 + \lambda q_1 \tag{4a}$$

where

$$\lambda = R\delta_0/(R-R'). \tag{5}$$

Similarly,

$$r' = r_0 - \lambda q_1. \tag{4b}$$

The parameter λ will be termed the effective conicity, for if the wheels were conical λ would be equal to the cone angle. Equation (5) is due to Heumann [9]; equations (3) and (5) were also derived by de Pater [15].

The normal reactions at the contact points, N and N', are given by

$$N = -\frac{1}{2l}\left(mr_0\ddot{q}_1 + 2d_2r_0\dot{q}_1 + 2k_2r_0q_1 - Wl\right),$$

$$N' = \frac{1}{2l}\left(mr_0\ddot{q}_1 + 2d_2r_0\dot{q}_1 + 2k_2r_0q_1 + Wl\right),$$

where W is the axle load. The lateral resultant of these normal reactions is

$$\begin{aligned} &N'\delta' - N\delta \\ &= -W\varepsilon q_1/l \end{aligned}$$

representing a restoring force, as is obvious on physical grounds.

The forces acting in the contact plane arise from the phenomenon of creep and will be assumed to consist of a longitudinal and a lateral component. The longitudinal force acting on the wheel can be expressed as $-f\gamma$ where f is the longitudinal creep coefficient and γ is the longitudinal creepage, defined by Carter [2] to be

$$\gamma = \frac{\text{actual forward displacement} - \text{pure rolling forward displacement}}{\text{forward displacement due to rolling}}.$$

Similarly, the lateral force acting on the wheel can be expressed as $-f'\gamma'$ where f' is the lateral creep coefficient and γ' is the lateral creepage

$$\gamma' = \frac{\text{actual lateral displacement} - \text{pure rolling lateral displacement}}{\text{forward displacement due to rolling}}.$$

The relationship between the creepage and the creep forces has been investigated for a variety of practical situations. Carter [16] gave a solution to the creep problem for the two-dimensional case of two long cylinders, pressed together by a normal force, and transmitting a tangential force across the contact strip. Similar results were obtained by Poritsky [17], and in the discussion of [17], Cain [18] pointed out that the region of adhesion must lie at the leading edge of the contact area. A three-dimensional case was solved approximately by Johnson [19] who considered an elastic sphere rolling on an elastic plane. This solution was based on the assumption that the area of adhesion is circular and tangential to the area of contact (which is also circular) at the leading edge. Reasonably good agreement with experiment was obtained. The influence of spin about an axis normal to the contact area has also been studied by Johnson [20]. De Pater [21] has also investigated the case where the contact area is circular, and derived solutions for both small and large creepages, without making assumptions about the shape of the area of adhesion. However, this analysis was confined to the case where Poisson's ratio was zero; Kalker [22] has given a complete analytical treatment for the case in which Poisson's ratio is not zero. The agreement between these theoretical results and the experimental results of Johnson [19] is very good. The general case where the contact area is elliptical has been considered by Haines and Ollerton [23] who confine their attention to creep in the direction of motion and assume that Carter's two-dimensional stress distribution holds in strips parallel to the direction of motion. A general theory for the elliptical contact area, based on similar assumptions to those made in [19], has been developed by Vermeulen and Johnson [24], yielding the relationship between creepages and tangential forces for arbitrary values of the ratio of the semi-axes of the contact area.

According to the solution given by Vermeulen and Johnson [24] the creep functions are given by the expressions

$$f = G\pi ab/\Phi,$$
$$f' = G\pi ab/\psi_1,$$

where G is the modulus of rigidity, $2a$ is the length of the contact area in the direction of rolling and $2b$ is the length of the contact area transverse to the direction of rolling. The functions Φ and ψ_1 depend on a/b and Poisson's ratio only, and have been derived and plotted in [24]. The dimensions of the contact area are obtained from the relations due to Hertz, and depend on the relative curvatures of wheel and rail and the normal reaction N. From [25],

$$\left(\frac{a}{m}\right)^3 = \left(\frac{b}{n}\right)^3 = \frac{3(1-\sigma)N}{2\left(\frac{1}{R}+\frac{1}{R'}+\frac{1}{r_0}\right)G}$$

where m, n are constants dependent on the curvatures, and σ is Poisson's ratio. Values for m, n are tabulated in [25]. The creep coefficients are proportional to $N^{2/3}$, and in the case where the contact area is circular, $a/b = 1$, and

$$\Phi = \pi(4-3\sigma)/16,$$
$$\psi_1 = \pi(4-\sigma)/16.$$

It will be assumed in the present analysis that the effect of variation of the normal reaction due to the motion of the wheelset has a negligible effect on the value of the creep coefficients.

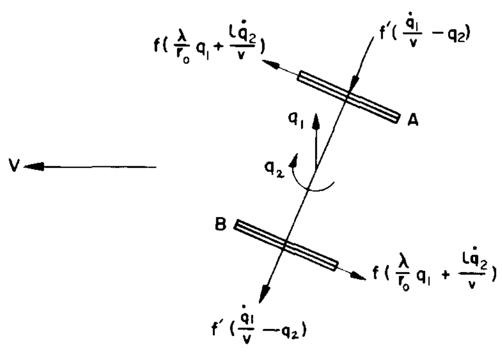

FIG. 3. Creep forces acting on wheelset.

A forward motion of the wheelset in a small interval of time results in the following displacements at the wheel tread in the longitudinal and lateral directions respectively, for wheel A (Fig. 3)

$$V\,dt - l\,dq_2, \qquad dq_1,$$

and for wheel B

$$V\,\mathrm{d}t+l\,\mathrm{d}q_2, \qquad \mathrm{d}q_1.$$

Because δ_0 is considered small, the difference between the lateral displacement of the wheelset at the centre of mass and at the treads due to tilting of the wheelset is neglected. The corresponding components of rolling displacements are, for wheel A

$$(r_0+\lambda q_1)V\,\mathrm{d}t/r_0, \qquad q_2 V\,\mathrm{d}t,$$

and for wheel B

$$(r_0-\lambda q_1)V\,\mathrm{d}t/r_0, \qquad q_2 V\,\mathrm{d}t.$$

It follows that the creepages are, for wheel A

$$\gamma = -\frac{\lambda}{r_0}q_1-\frac{l}{V}\dot{q}_2, \qquad \gamma' = \frac{\dot{q}_1}{V}-q_2, \tag{6}$$

and for wheel B

$$\gamma = \frac{\lambda}{r_0}q_1+\frac{l}{V}\dot{q}_2, \qquad \gamma' = \frac{\dot{q}_1}{V}-q_2. \tag{7}$$

The generalized forces Q_1 and Q_2 can now be written down in the form

$$Q_1 = -\frac{2f'\dot{q}_1}{V}+2f'q_2-W\varepsilon\frac{q_1}{l}, \qquad Q_2 = -\frac{2fl^2\dot{q}_2}{V}-\frac{2f\lambda l}{r_0}q_1. \tag{8}$$

Substituting from equations (8) into equations (1) and defining the following non-dimensional quantities

$$\mu = 2fl/mV_0^2, \qquad \mu' = 2f'l/mV_0^2,$$

$$\alpha = \lambda l/r_o, \qquad v = V/V_0, \qquad s = \frac{l}{V_0}\frac{\mathrm{d}}{\mathrm{d}t},$$

$$j = C/ml^2, \qquad \zeta_1 = 2d_1 d/mV_0, \qquad \zeta_2 = 2d_2 l/mV_0,$$

$$\varepsilon_1 = 2k_1 d^2/mV_0^2, \qquad \varepsilon_2 = 2k_2 l^2/mV_0^2, \qquad \bar{\varepsilon}_2 = W\varepsilon l/mV_0^2,$$

$$\phi_1 = q_1/l, \qquad \phi_2 = q_2, \qquad \bar{\bar{\varepsilon}}_2 = \varepsilon_2+\bar{\varepsilon}_2,$$

where V_0 is a reference velocity, the equations of motion take the form

$$\left[s^2+\left(\frac{\mu'}{v}+\zeta_2\right)s+\bar{\bar{\varepsilon}}_2\right]\phi_1-\mu'\phi_2 = 0, \qquad \mu\alpha\phi_1+\left[js^2+\left(\frac{\mu}{v}+\zeta_1\right)s+\varepsilon_1\right]\phi_2 = 0. \tag{9}$$

The non-conservative nature of the system is indicated by the assymmetry of the coupling terms due to creep and conicity. It is due to this property that dynamic instability can occur.

Some typical values are

$$r_0 = 1{\cdot}75\ \text{ft}, \qquad l = 2{\cdot}5\ \text{ft}, \qquad d = 3{\cdot}25\ \text{ft},$$

$$m = 90\ \text{slugs}, \qquad C = 360\ \text{slugs ft}^2, \qquad W = 9300\ \text{lb},$$

$$k_1 = k_2 = 5000\ \text{lb/ft}, \qquad f = f' = 3\times 10^6\ \text{lb},$$

$$R' = 0{\cdot}690\ \text{ft}, \qquad R = 0{\cdot}787\ \text{ft}, \qquad \delta_0 = 0{\cdot}05,$$

and taking the reference velocity $V_0 = 100$ ft/sec it follows that

$$\mu = \mu' = 16{\cdot}7 \qquad \alpha = 0{\cdot}571, \qquad j = 0{\cdot}640,$$

$$\varepsilon_1 = 0{\cdot}1176, \qquad \varepsilon_2 = 0{\cdot}0694, \qquad \bar{\varepsilon}_2 = 0{\cdot}6562.$$

These numerical values will be used to illustrate the theory as it is developed.

KINEMATIC OSCILLATIONS OF WHEELSETS

Before considering the stability of the elastically restrained wheelset it is useful to consider the behaviour of an unrestrained wheelset in motion at a low forward speed. The theory appears to have been first given by Klingel [4]; it is also discussed by Carter [2].

As the wheelset is unrestrained, the elastic suspension stiffnesses will be zero. To obtain the solution of Carter it is also necessary to neglect the gravitational stiffness terms which were not included in Carter's analysis. Also neglecting the inertia terms, the equations of motion reduce to

$$\frac{\mu' s}{v}\phi_1 - \mu'\phi_2 = 0,$$

$$\mu\alpha\phi_1 + \frac{\mu s}{v}\phi_2 = 0.$$

Elimination of ϕ_1 and ϕ_2 yields

$$s^2 = -\alpha v^2$$

indicating that the motion has a single undamped oscillatory constituent with frequency ν given by

$$\nu^2 = \alpha v^2. \tag{10}$$

In dimensional terms, the frequency is

$$\omega = V\sqrt{\frac{\lambda}{r_0 l}}$$

and is therefore proportional to the forward speed of the wheelset.

The motion of the wheelset in this mode is

$$\phi_1 = -a_1 \cos \nu t,$$
$$\phi_2 = a_2 \sin \nu t,$$

where

$$\left(\frac{a_2}{a_1}\right)^2 = \alpha.$$

This motion is independent of the values of the creep coefficients, because it is a case of pure rolling and the creepages γ and γ' are zero at every instant during the motion.

As the frequency is proportional to speed the neglect of the inertia terms is seen to be appropriate for very low forward speeds. For the typical wheelset, the parameters of which were given above, the wavelength of the kinematic oscillation is 20·8 ft. For coned wheels, $\delta_0 = 0{\cdot}05$, the wavelength is 58·8 ft.

APPROXIMATE ROOT LOCUS FOR THE ELASTICALLY RESTRAINED WHEELSET

In the absence of suspension damping, the effect of which will be discussed later, the equations of motion take the form

$$\left(s^2+\frac{\mu'}{v}s+\bar{\bar{\varepsilon}}_2\right)\phi_1-\mu'\phi_2 = 0,$$

$$\mu\alpha\phi_1+\left(js^2+\frac{\mu}{v}s+\varepsilon_1\right)\phi_2 = 0. \tag{11}$$

For a free motion of the type

$$q_r = K_r e^{\lambda t},$$

the characteristic equation of the system is

$$p_4\lambda^4+p_3\lambda^3+p_2\lambda^2+p_1\lambda+p_0 = 0, \tag{12}$$

where

$$p_4 = j,$$

$$p_3 = \frac{1}{v}(\mu' j+\mu),$$

$$p_2 = j\bar{\bar{\varepsilon}}_2+\varepsilon_1+\frac{\mu\mu'}{v^2},$$

$$p_1 = \frac{1}{v}(\mu'\varepsilon_1+\mu\bar{\bar{\varepsilon}}_2),$$

$$p_0 = \varepsilon_1\bar{\bar{\varepsilon}}_2+\mu\mu'\alpha.$$

Typical solutions of this quartic equation show that it possesses a pair of real roots with relatively large values, and a pair of complex roots with relatively small modulus. Due to the large difference in size of the moduli, an approximation to the larger roots is given by equating to zero the first three terms of the characteristic equation. An approximation to the quartic then takes the form

$$\left(p_4\lambda^2+p_3\lambda+p_2\right)\left(\lambda^2+\frac{p_2p_1-p_3p_0}{p_2^2}\lambda+\frac{p_0}{p_2}\right) = 0 \tag{13}$$

which is chosen so that the coefficients of the terms in λ of order one and zero of the quartic shall have their correct values. Because, in most practical applications, the magnitude of the creep coefficients is large in relation to the inertia and stiffness coefficients, a further approximation consisting of writing

$$p_2 = \frac{\mu\mu'}{v^2},$$

$$p_0 = \mu\mu'\alpha,$$

is made. Accordingly, equation (13) can be further factorised and written as

$$(\lambda+\eta_1)(\lambda+\eta_2)(\lambda^2+2\eta_3\lambda+\nu_3^2) = 0,$$

where

$$\eta_1 = \frac{\mu'}{v},$$

$$\eta_2 = \frac{\mu}{jv},$$

$$\eta_3 = \frac{(j\mu'+\mu)v}{2\mu\mu'}\left[\left(\frac{\mu'\varepsilon_1+\mu\bar{\bar{\varepsilon}}_2}{\mu'j+\mu}\right)-\alpha v^2\right],$$

$$\nu_3^2 = \alpha v^2.$$

The two real roots $\lambda = -\eta_1$ and $\lambda = -\eta_2$ correspond to heavily damped subsidences. The former subsidence is associated with a motion in which only lateral translation of the wheelset takes place, yawing of the wheelset being negligible to the present approximation. Similarly, the latter subsidence refers to a motion in which yawing of the wheelset is predominant, lateral translation being negligible. The quadratic factor yields a conjugate complex pair of roots on solution, corresponding to an oscillatory motion. The frequency ν_3 of this oscillation is the same as the frequency of the kinematic oscillation, equation (10). The damping of the oscillation is positive at low speeds, and as the speed is increased it reaches a maximum and then decreases until it vanishes at a critical speed v_0 given by

$$v_0^2 = \frac{1}{\alpha}\left(\frac{\mu'\varepsilon_1+\mu\bar{\bar{\varepsilon}}_2}{j\mu'+\mu}\right). \tag{14}$$

The damping is negative at higher speeds, and the system is therefore unstable. The critical speed is inversely proportional to the square root of the conicity α, and therefore becomes infinite when the effective conicity is zero—a result to be expected as the lateral translation and yawing modes of the wheelset are then uncoupled. Overall increases of stiffness are stabilising and overall increases in inertia are destabilising. The frequency at which instability occurs, ν_c, is given by

$$\nu_c^2 = \left(\frac{\mu'\varepsilon_1+\mu\bar{\bar{\varepsilon}}_2}{j\mu'+\mu}\right). \tag{15}$$

Comparison of (14) and (15) shows that the system is unstable when the kinematic frequency exceeds the frequency given by (15), as illustrated by Fig. 4, which shows the behaviour of the oscillatory root as the speed varied. For the example wheelset the critical speed is 94·9 ft/sec, and the critical frequency is 4·56 c/s.

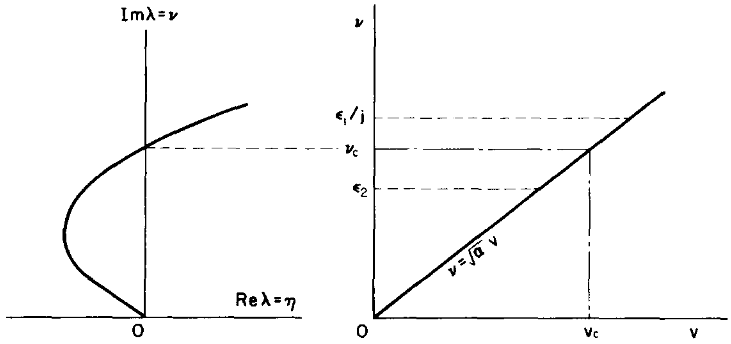

FIG. 4. Behaviour of oscillatory root for elastically restrained wheelset as speed is raised.

The maximum damping factor occurs at low speeds and is

$$\left.\frac{\eta_3}{\nu_3}\right|_{v\to 0} = \frac{1}{2\sqrt{\alpha}}\left(\frac{\varepsilon_1}{\mu}+\frac{\bar{\bar{\varepsilon}}_2}{\mu'}\right).$$

For the example wheelset, the maximum damping factor is only 0·0334.

EXACT TREATMENT OF WHEELSET INSTABILITY

The approximate solution derived above is useful in indicating the behaviour of the system at various speeds. If attention is restricted to the motion at the critical speed, an exact analysis of the system is possible.

At the critical speed, the motion is sinusoidal and the characteristic equation (12) may be replaced by the two conditions

$$\nu_c^2 = \frac{p_1}{p_3}, \tag{16}$$

$$p_4\nu_c^4 - p_2\nu_c^2 + p_0 = 0.$$

The elimination of the critical frequency between these two equations yields Routh's discriminant for the system. The first of equations (16) yields equation (15), so that the critical frequency given by the approximate factorization of the characteristic equation is, in fact, exact. The second of equations (16) yields, after some reduction, an expression for the critical speed v_c which, in terms of the approximate critical speed v_0 given by equation (14) is,

$$v_c^2 = v_0^2\left[\frac{1}{1-\frac{1}{\alpha}\left(\frac{\varepsilon_1 - j\bar{\varepsilon}_2}{\mu' j + \mu}\right)^2}\right]. \tag{17}$$

Equation (17) shows that the approximate value for the critical speed will be accurate provided that either the creep coefficients are very large in relation to the elastic stiffnesses or that the modal frequencies are sufficiently close.

The motion of the system, in the mode in which the damping is zero at the critical speed will take the form

$$\begin{aligned} \phi_1 &= a_1 \sin(v_c t + \theta), \\ \phi_2 &= a_2 \sin v_c t, \end{aligned} \tag{18}$$

so that θ is the phase lag of yaw behind lateral translation and a_1 and a_2 are relative amplitudes. Substituting from (18) into the equations of motion yields the relationships

$$\begin{aligned} \sin\theta &= -\frac{a_2 v_c}{v_c \alpha a_1}, \\ \cos\theta &= \frac{j v_c^2 a_2 - \varepsilon_1 a_2}{\mu \alpha a_1}. \end{aligned} \tag{19}$$

Eliminating the amplitude ratio a_2/a_1 from (19) gives

$$\tan\theta = \frac{-v_c \mu}{v_c (j v_c^2 - \varepsilon_1)}, \tag{20}$$

or, equivalently using (15),

$$\tan\theta = \frac{v_c \mu}{v_c (v_c^2 - \bar{\varepsilon}_2)}. \tag{21}$$

Now, equation (15) shows that the critical frequency lies between the modal frequencies which are equal to $\bar{\varepsilon}_2$ and ε_1/j. If ε_1/j is greater than $\bar{\varepsilon}_2$, $\tan\theta$ is positive, but if ε_1/j is less than $\bar{\varepsilon}_2$, $\tan\theta$ is negative. Normally, the creep coefficients μ and μ' are large relative to the inertia and stiffness coefficients, and then θ will be slightly less than $-90°$ if ε_1/j is greater than $\bar{\varepsilon}_2$ and slightly greater than $-90°$ if ε_1/j is less than $\bar{\varepsilon}$.

Eliminating θ from equations (19), the amplitude ratio is found to be

$$\left(\frac{a_2}{a_1}\right)^2 = \alpha. \tag{22}$$

The amplitude ratio is therefore identical to that found in the kinematic mode of the slowly rolling, unrestrained wheelset.

The motion in the critical mode is therefore closely similar to that of a slowly rolling, unrestrained wheelset. In the case of the example wheelset the phase angle θ is $-89{\cdot}04°$.

ENERGY BALANCE AT THE CRITICAL SPEED

Let P represent the tractive force acting on the wheelset in the longitudinal direction and M the tractive torque. The axis of the torque vector, lies along the centre-line of the axle. Then, referring to Fig. 5, for equilibrium we have to the second order in the generalized coordinates

$$\begin{aligned} P &= -\mu'\phi_2\left(\frac{s\phi_1}{v}-\phi_2\right), \\ M &= \frac{r_0}{l}\mu\alpha\phi_1\left(\alpha\phi_1+\frac{s\phi_2}{v}\right). \end{aligned} \tag{23}$$

The longitudinal force arises from the lateral creep forces and the torque arises from the longitudinal creep forces. The elastic and inertia forces have no resultant in the longitudinal direction. (The tractive forces P and M represent the incremental values due to the lateral motion.)

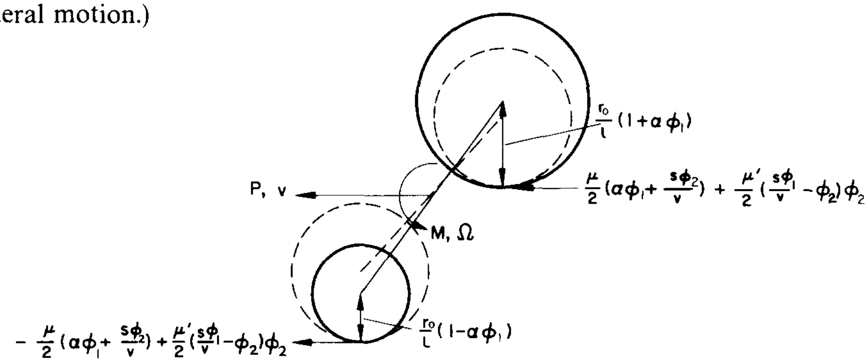

FIG. 5. Resultant longitudinal forces and tractive forces acting on wheelset.

The kinetic energy T of the system is

$$T = \tfrac{1}{2}s^2\dot{\phi}_1^2+\tfrac{1}{2}js^2\dot{\phi}_2^2, \tag{24}$$

and the total potential energy V, arising from the strain energy of the suspension and the gravitational potential energy is

$$V = \tfrac{1}{2}\bar{\bar{\varepsilon}}_2\phi_1^2+\tfrac{1}{2}\varepsilon_1\phi_2^2. \tag{25}$$

Introducing a dissipation function F for the creep forces, analogous to Rayleigh's dissipation function, equal to half the rate of energy dissipation, which is for two wheels

$$F = \tfrac{1}{2}\mu v\gamma^2+\tfrac{1}{2}\mu' v\gamma'^2. \tag{26}$$

The equation of energy balance is

$$\frac{\mathrm{d}}{\mathrm{d}t}(T+V)+2F-Pv-M\Omega = 0, \tag{27}$$

where Ω is the constant (non-dimensional) angular velocity of the wheelset. On substitution from (23), (26) and (6) and (7) the energy balance equation becomes

$$\frac{\mathrm{d}}{\mathrm{d}t}(T+V)+\mu\dot{\phi}_2\left(\alpha\phi_1+\frac{\dot{\phi}_2}{v}\right)+\mu'\dot{\phi}_1\left(\frac{\dot{\phi}_1}{v}-\phi_2\right) = 0. \tag{28}$$

This equation can also be obtained by multiplying the first of equations (11) by $\dot{\phi}_1$, the second of equations (11) by $\dot{\phi}_2$ and adding. Equation (27) clearly shows that the source of energy which promotes the active behaviour of the system is the tractive effort.

At the critical speed, and considering only the critical mode, equation (27) may be integrated over one complete cycle of the oscillation. Since the kinetic and potential energies have the same values at the end of the cycle as they had at the beginning of the cycle, we have

$$2\int_0^T F\,dt - v\int_0^T P\,dt - \Omega\int_0^T M\,dt = 0 \tag{29}$$

where $T = 2\pi/\nu_c$. On substitution from equations (18)

$$2\int_0^T F\,dt = \frac{\mu v\pi}{\nu_c}\left(\frac{a_2^2\nu_v^2}{v^2} + \alpha^2 a_1^2 + \frac{2\alpha a_1 a_2 \nu_c}{v}\sin\theta\right) + \\ + \frac{\mu' v\pi}{\nu_c}\left(\frac{a_1^2\nu_c^2}{v^2} + a_2^2 + \frac{2a_1 a_2 \nu_c}{v}\sin\theta\right), \tag{30}$$

and

$$v\int_0^T P\,dt + \Omega\int_0^T M\,dt = \frac{\mu\alpha a_1 v\pi}{\nu_c}\left(\alpha a_1 + \frac{a_2\nu_c}{v}\sin\theta\right) + \frac{\mu'\pi a_2 v}{\nu_c}\left(\frac{a_1\nu_c}{v}\sin\theta + a_2\right), \tag{31}$$

so that the equation of energy balance (29) reduces to

$$(\mu' + \mu\alpha)a_2 a_1 \sin\theta + \nu\left(\frac{\mu'}{v}a_1^2 + \frac{\mu}{v}a_2^2\right) = 0. \tag{32}$$

The first term in equation (32) arises from the stiffness coupling terms due to creep and conicity. The second term represents the dissipation of energy by the creep damping terms. It is easily verified that equation (32) is satisfied identically by equations (19) and (22).

Though the motion at the critical speed has constant amplitude, energy is being continuously dissipated by the action of creep. The rate of dissipation of energy is given by equation (30) and is, of course, equal to the energy supplied by the tractive effort given by equation (31). Eliminating the phase angle θ by means of equation (19) and the yaw amplitude a_2 with equation (22) we find that the energy dissipated in one cycle is

$$2\int_0^T F\,dt = \frac{\pi v_c}{\nu_c}\left(\alpha - \frac{\nu_c^2}{v_c^2}\right)\left(\mu\alpha + \mu'\right)a_1^2,$$

or, eliminating ν_c and v_c using equations (15) and (17)

$$2\int_0^T F\,dt = \frac{\pi v_c}{\sqrt{(\alpha v_0)}}\left(\frac{\varepsilon_1 - j\bar{\bar{\varepsilon}}_2}{\mu' j + \mu}\right)^2(\mu\alpha + \mu')a_1^2. \tag{33}$$

This depends on the separation of the modal frequencies; if they are equal, the dissipation per cycle is zero, for in this case the mode of instability is the same as the kinematic mode and there is no creepage.

EFFECTS OF VARIOUS PARAMETERS ON STABILITY

The effects of varying the ratio of the creep coefficients μ/μ' follow from inspection of equations (14) and (15). Assuming that both μ and μ' are large in comparison with the elastic and inertia coefficients, v_0 is a good approximation to the critical speed and as

$$\mu/\mu' \to 0, \qquad v_c^2 \to \frac{\varepsilon_1}{j}, \qquad v_0^2 \to \frac{\varepsilon_1}{j\alpha}.$$

If the ratio μ/μ' is increased then as

$$\mu/\mu' \to \infty, \qquad v_c^2 \to \bar{\bar{\varepsilon}}_2, \qquad v_0^2 \to \bar{\bar{\varepsilon}}_2/\alpha.$$

Thus, if ε_1/j is greater than $\bar{\bar{\varepsilon}}_2$ increasing the ratio μ/μ' is destabilizing, but if $\bar{\bar{\varepsilon}}_2$ is greater than ε_1/j increasing the ratio μ/μ' is stabilizing. The results obtained by Johnson [24] indicate that the maximum ratio of the creep coefficients f/f' occurs when the ellipticity a/b of the contact area tends to zero and is then equal to 1·4. As a/b is increased, f/f' is reduced and tends to unity as a/b becomes very large.

Variations of the creep coefficients μ and μ', their ratio being kept constant, do not have any effect on the critical frequency. For large values of the creep coefficients, the critical speed represented by v_0 is similarly unaffected by the magnitude of the creep coefficients. For sufficiently low values of μ and μ' equation (17) shows that reduction of the value of the creep coefficients increases the critical speed and when the inequality

$$\left(\frac{\varepsilon_1 - j\bar{\bar{\varepsilon}}_2}{\mu' j + \mu}\right)^2 > \alpha$$

is satisfied, the system is stable at all speeds. The variation of critical speed with creep coefficient, when $\mu = \mu'$, is shown in Fig. 6. In this case it is particularly noteworthy

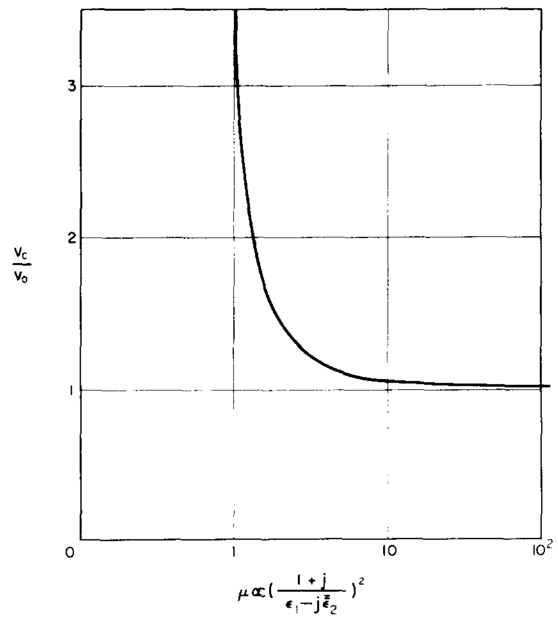

FIG. 6. Variation of critical speed of elastically restrained wheelset with creep coefficient $\mu = \mu'$.

that extremely large variations in the creep coefficient have negligible effect on the critical speed. It has been shown above that the damping of the oscillatory mode is inversely proportional to the creep coefficient and as this coefficient is increased in value, the damping is reduced and the motion more nearly corresponds to that in the kinematic mode. In the limit, the system behaviour is similar to that of a system subject to non-holomonic constraints. Figure 7 shows, in diagrammatic form, the root locus for the system at a

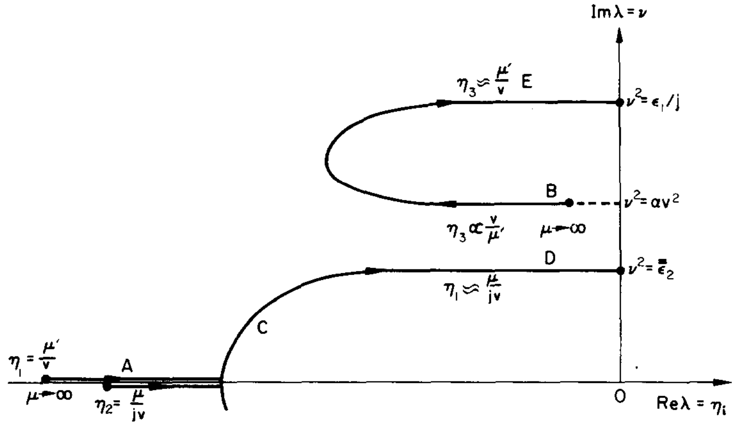

FIG. 7. Root locus for elastically restrained wheelset as creep coefficient $\mu = \mu'$ is varied from zero to infinity.

given forward speed as the creep coefficients are varied from zero to very large values. For large values of the creep coefficient the approximate theory is valid and the roots of the characteristic equation lie on the sectors A and B. As the creep coefficient is reduced in value, the two real roots become equal at C and further reductions in creep coefficient yield a complex, conjugate pair of roots, corresponding to a damped oscillation. For small values of the creep coefficient the roots lie on sectors D and E. As explained above, the system is stable and the two damped oscillations correspond to the uncoupled modes of oscillation of the wheelset, lateral translation and yaw, with frequencies ε_1/j and $\bar{\bar{\varepsilon}}_2$. For these oscillations the damping in each mode is proportional to the creep coefficient. The stability of the system when the creep coefficients are small can be determined by an analysis identical to that employed by Bolotin [1] in the case of other non-conservative systems, but this aspect will not be pursued any further.

The effect of the combined geometry of wheel tread and rail head on stability can be traced by considering equation (14) in conjunction with equations (4) and (5). Defining a parameter

$$\mathscr{F} = Wl^2/mV_0^2R',$$

the critical speed is given by the expression

$$V_0^2 = \frac{r_0}{\delta_0 l(\mu' j + \mu)}\left[\mu'\varepsilon_1 + \mu\varepsilon_2 + (\mathscr{F}\mu - \mu\varepsilon_2 - \mu'\varepsilon_1)\frac{R'}{R}\right]. \tag{34}$$

For a given rail head radius, decreasing the radius of curvature of the wheel tread is stabilizing if (Fig. 8)

$$\mathscr{F} > \varepsilon_2 + \frac{\mu'}{\mu}\varepsilon_1. \tag{35}$$

Thus, decreasing the radius of curvature of the wheel tread increases the critical speed if the axle-load is sufficiently large, or if the suspension stiffnesses are sufficiently small as indicated by the inequality, equation (35). This inequality reflects the competing roles of effective conicity and of gravitational stiffness, both of which depend on the geometry of rail and wheel. Increasing the slope of the contact plane, δ_0, decreases the critical speed. The limiting case when $R = R'$, though giving a finite critical speed, is not a realistic condition as the gravitational stiffness is infinite and lateral displacement is prevented.

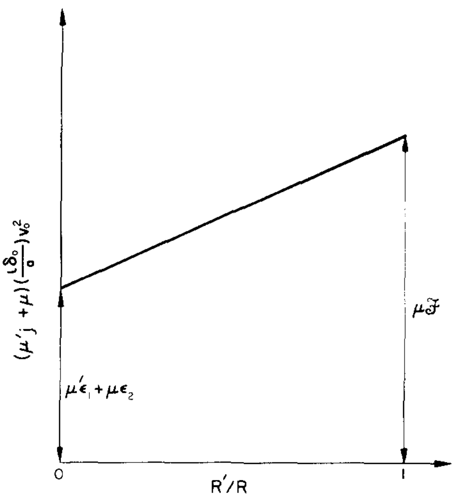

FIG. 8. Variation of critical speed with ratio of radius of curvature of rail head to radius of curvature of wheel tread.

It has been found in practice that wheels which initially possess conical treads are rapidly worn so that the treads become concave. During the wearing process, the slope of the contact plane δ_0 remains constant, but the radius of curvature of the wheel tread decreases rapidly until a profile is obtained which is not subject to any further change. For the example wheelset, reduction in the radius of curvature of the wheel tread increases the effective conicity from 0·05 (the value of δ_0) when the radius is infinite to 0·40 when the radius is 0·787 ft; the latter corresponds to a profile of a fully worn wheel, and the rail head radius is, as specified above, 0·690 ft. The increase in lateral stiffness due to curvature of the wheel tread raises the natural frequency of the lateral translation mode of the wheelset from 1·68 c/s to 5·45 c/s, and the corresponding variation of critical speed is from 151 ft/sec to 94·9 ft/sec, indicating that in this case the destabilizing effect of the increased effective conicity is only partly offset by the stabilizing effect of increased lateral stiffness.

INFLUENCE OF SUSPENSION DAMPING ON STABILITY

In order to avoid algebraic complexities, the qualitative effects of the influence of suspension damping on stability can be discussed using the effective conicity α as the parameter descriptive of the stability of the system, for it has been established above that, for the system with no suspension damping, increasing α reduces the critical speed and reducing α increases the critical speed. Therefore, consider the equations of motion

$$\begin{aligned} (s^2+\delta_2 s+\varepsilon_2)\phi_1-\mu'\phi_2 &= 0, \\ \mu\alpha\phi_1+(js^2+\delta_1 s+\varepsilon_1)\phi_2 &= 0, \end{aligned} \qquad (36)$$

where

$$\delta_1 = \frac{\mu}{v}+\zeta_1,$$

$$\delta_2 = \frac{\mu'}{v}+\zeta_2.$$

The characteristic equation of this system of equations is

$$p_4\lambda^4+p_3\lambda^3+p_2\lambda^2+p_1\lambda+p_0 = 0,$$

where

$$\begin{aligned} p_4 &= j, \\ p_3 &= \delta_2 j+\delta_1, \\ p_2 &= j\bar{\bar{\varepsilon}}_2+\varepsilon_1+\delta_1\delta_2, \\ p_1 &= \delta_2\varepsilon_1+\delta_1\bar{\bar{\varepsilon}}_2, \\ p_0 &= \bar{\bar{\varepsilon}}_2\varepsilon_1+\mu\mu'\alpha. \end{aligned}$$

As before, the critical frequency is given by

$$v_c^2 = \frac{p_1}{p_3} = \frac{\delta_2\varepsilon_1+\delta_1\bar{\bar{\varepsilon}}_2}{\delta_2 j+\delta_1}, \qquad (37)$$

and the critical value of α is given by Routh's discriminant

$$p_4p_1^2-p_2p_1p_3+p_0p_3^2 = 0,$$

which gives, after some reduction,

$$\alpha_c = \frac{\delta_1\delta_2}{\mu\mu'(\delta_2 j+\delta_1)^2}\left[(\varepsilon_1-\bar{\bar{\varepsilon}}_2 j)^2+\delta_1^2\varepsilon_2+\delta_1\delta_2(j\bar{\bar{\varepsilon}}_2+\varepsilon_1)+\delta_2^2 j\varepsilon_1\right].$$

Writing $\delta_1 = \delta$, $\delta_2 = \eta\delta$, this reduces to

$$\alpha_c = \frac{\eta}{\mu\mu'(j\eta+1)^2}\left\{(\varepsilon_1-\bar{\bar{\varepsilon}}_2 j)^2+\delta^2\left[\bar{\bar{\varepsilon}}_2+\eta(j\bar{\bar{\varepsilon}}_2+\varepsilon_1)+\eta^2 j\varepsilon_1\right]\right\}.$$

Normally, the creep coefficients will be large compared with the elastic and inertia coefficients, and the term $(\varepsilon_1-\varepsilon_2 j)$, proportional to the difference of the squares of the modal frequencies, may be neglected. Then

$$\alpha_c = \frac{\eta\delta^2}{\mu\mu'}\left(\frac{\bar{\bar{\varepsilon}}_2+\varepsilon_1\eta}{1+j\eta}\right) \tag{38}$$

which reduces to equation (14) if the suspension dampings ζ_1 and ζ_2 are made zero. Since, from (37) the critical frequency ν_c is given by

$$\nu_c^2 = \frac{\bar{\bar{\varepsilon}}_2+\varepsilon_1\eta}{1+j\eta},$$

we have the relationship

$$\alpha_c = \frac{\delta_1\delta_2}{\mu\mu'}\nu_c^2. \tag{39}$$

Noting that the critical frequency depends only on the ratio of the damping coefficients, equation (39) shows that if the suspension damping is increased in the same proportion as the creep damping the critical value of the conicity is increased and the system is therefore more stable.

The effect of adding suspension damping is made more clear by considering the free motion of an unrestrained wheelset subject to viscous damping forces. The equations of motion for this system will be

$$\left(\frac{\mu'}{v}+\zeta_2\right)s\phi_1-\mu'\phi_2 = 0,$$

$$\mu\alpha\phi_1+\left(\frac{\mu}{v}+\zeta_1\right)s\phi_2 = 0,$$

which yields a single undamped oscillatory constituent with frequency, in the notation used above.

$$\nu^2 = \frac{\mu\mu'\alpha}{\delta_1\delta_2}. \tag{40}$$

Thus, in this case, the effect of adding suspension damping is to reduce the frequency of the kinematical oscillation at a given speed. Since in practical cases, the amount of suspension damping which can be provided is likely to be small in comparison with the damping provided by creepage, the effect on the kinematical frequency is likely to be small at ordinary speeds.

APPLICATION OF THE THEORY TO BOGIES

The theory developed above can be extended at once to cover the case of a bogie which consists of two wheelsets mounted in a rigid bogie frame without lateral or longitudinal clearance or flexibility, Fig. 1. The equations of motion become

$$\begin{aligned} \left(\gamma s^2+\frac{2\mu'}{v}s+\varepsilon_2^*\right)\phi_1-2\mu'\phi_2 &= 0,\\ 2\mu\alpha\phi_1+\left(\bar{j}s^2+\frac{2\bar{\mu}}{v}s+\varepsilon_1^*\right)\phi_2 &= 0, \end{aligned} \tag{41}$$

where ϕ_1 refers to lateral displacement of the bogie and ϕ_2 to yaw of the bogie; the bogie wheelbase is $2\beta l$ and

$$\bar{\mu} = \mu + \mu'\beta^2,$$
$$\varepsilon_1^* = \varepsilon_1 + 2\varepsilon_2\beta^2,$$
$$\varepsilon_2^* = \varepsilon_2 + 2\varepsilon_2,$$

and γ and $\bar{j}$ are the non-dimensional mass and moment of inertia in yaw of the complete bogie. All other symbols are used in the same sense as previously. A similar analysis to that given for the elastically restrained wheelset yields the approximate expression for the critical speed in the case where the creep coefficients are large compared with the elastic and inertia coefficients

$$v_0^2 = \frac{\bar{\mu}}{\mu\alpha}\left(\frac{\mu'\varepsilon_1^* + \bar{\mu}\varepsilon_2^*}{\bar{j}\mu' + \gamma\bar{\mu}}\right), \tag{42}$$

and the critical frequency is given by

$$\nu_c^2 = \left(\frac{\mu'\varepsilon_1^* + \bar{\mu}\varepsilon_2^*}{\bar{j}\mu' + \gamma\bar{\mu}}\right). \tag{43}$$

The frequency of the kinematic oscillation of the bogie is given by

$$\nu^2 = \frac{\mu}{\bar{\mu}}\alpha v^2, \tag{44}$$

or in dimensional terms the well-known expression [2]

$$\omega = V\sqrt{\left[\frac{\lambda}{r_0 l(1+\beta^2)}\right]}.$$

Some typical values for a bogie are as follows:

$r_0 = 1{\cdot}75$ ft,	$l = 2{\cdot}5$ ft,	$d = 3{\cdot}25$ ft,
$\gamma m = 400$ slugs,	$\bar{j}ml^2 = 6000$ slugs ft^2,	$W = 9300$ lb,
$k_1 = k_2 = 20{,}000$ lb/ft,	$R = 0{\cdot}787$ ft,	$f = f' = 3 \times 10^6$ lb,
$R' = 0{\cdot}690$ ft,	$\beta = 1{\cdot}70$,	$\delta_0 = 0{\cdot}05$,

and taking $V_0 = 100$ ft/sec then

$\mu = \mu' = 16{\cdot}7$,	$\alpha = 0{\cdot}571$,	$\bar{j} = 10{\cdot}67$,
$\bar{\mu} = 65{\cdot}0$,	$\varepsilon_1 = 0{\cdot}470$,	$\varepsilon_2 = 0{\cdot}278$,
$\gamma = 4{\cdot}44$,	$\varepsilon_1^* = 4{\cdot}26$,	$\varepsilon_2^* = 1{\cdot}59$.

With these values the kinematic wavelength becomes 41·0 ft; with coned wheels, $\delta_0 = 0{\cdot}05$, the kinematic wavelength is 116 ft. Thus the wavelength for the bogie is almost twice that for a single wheelset. The critical speed is 160 ft/sec and the critical frequency is 3·89 c/s. With coned wheels the critical speed is 174 ft/sec, and the critical frequency is

1·50 c/s. The maximum damping factor occurs at low speeds and is given by

$$\left.\frac{\eta_3}{\nu_3}\right|_{v\to 0} = \tfrac{1}{2}\left(\frac{\bar{\mu}}{\mu\alpha}\right)^{\frac{1}{2}}\left(\frac{\varepsilon_1^*}{\bar{\mu}}+\frac{\varepsilon_2^*}{\mu'}\right).$$

For the example bogie the maximum damping factor is 0·210.

CONCLUDING REMARKS

Within the limits imposed by the assumption of small oscillations, the theory indicates that increases in suspension stiffness are effective in increasing the critical speed of the wheelset or bogie instability. This confirms the results of Carter [3], Rocard [5] and others for the case of bogies with coned wheels. Decreasing wheelset or bogie inertia also increases the critical speed. The magnitudes of the creep coefficients, and suspension damping have little effect on the critical speed in practical cases. The analysis given here indicates the importance of wheel tread wear, which may increase or reduce the critical speed, but which should be considered in estimating the suspension stiffness required for stability. An important feature of the results obtained here is the small amount of damping in the kinematic mode, particularly for the wheelset, which may be reflected in the response characteristics of the vehicle.

General conclusions regarding the stability of railway vehicles can only be drawn after the study of a complete vehicle in which the influence of the body freedoms is accounted for, and this matter will be considered in a sequel to this paper. However, the theory advanced here accounts for the main features of a particular form of instability experienced by railway vehicles.

Acknowledgement—Acknowledgement is made to the Chief of Research, British Rail Board, for permission to publish this paper and to D. L. Bartlett, Director of Engineering Research for his support of this study I am grateful to Dr. D. Williams for many helpful comments during the preparation of this paper.

REFERENCES

[1] V. V. BOLOTIN, *Nonconservative Problems of the Theory of Elastic Stability*. Pergamon Press, Oxford (1963).
[2] F. W. CARTER, *Railway Electric Traction*, pp. 57–70. Edward Arnold, London (1922).
[3] F. W. CARTER, *Proc. Roy. Soc.* **A121**, 585–611 (1928).
[4] KLINGEL, *Organ Fortschr. Eisenb. Wes.* **38**, 113–123 (1883).
[5] Y. ROCARD, *Actual. scient. ind.* **234** (1935); *General Dynamics of Vibrations*, pp. 306–312. Crosby Lockwood, London (1960).
[6] B. S. CAIN, *Vibration of Road and Rail Vehicles*, pp. 149–189. Pitman, New York (1940).
[7] R. D. DAVIES, *J. Instn civ. Engrs* **11**, 224–261 (1939).
[8] R. D. DAVIES and A. F. COOK, *Proc. Instn mech. Engrs* **158**, 426–434 (1948).
[9] H. HEUMANN, *Grundzüge der fuhrung der schienenfahrzeuge*, p. 133, Oldenbourg, München (1953).
[10] R. DE POSSEL and J. BEAUTEFOY, Papers awarded prizes in the competition sponsored by Office of Research and Experiment of the International Union of Railways. Utrecht (1960).
[11] C. T. MÜLLER, *Glasers Annln Gewerbe Bauw.* **82**, 31–47 (1958).
[12] R. P. BRANN, *On the Influence of Externally Applied Harmonic, Spring and Viscous Damping Forces to the Yawing Oscillations of a Simple Trolley Having Four Coned Wheels*. University College London, Mechanical Engineering Department, Report No. 62/1 (1962).
[13] T. MATSUDEIRA, Paper awarded prize in the competition sponsored by Office of Research and Experiment of the International Union of Railways. Utrecht (1960).
[14] A. D. DE PATER, *Appl. scient. Res. A.* **6**, 263–316 (1956); **10**, 205–228 (1961).
E. KATZ and A. D. DE PATER, *Appl. scient. Res. A.* **7**, 393–407 (1958).

[15] A. D. DE PATER, *Expose de la theorie de l'interaction entre le voie et le vehicule de chemin de fer. Mouvement sur une voie en alignment droit*. Universite Technique de Delft, Laboratoire de Mecanique Technique, Rapport No. 220.
[16] F. W. CARTER, *Proc. Roy. Soc.* **A112**, 151–157 (1926).
[17] H. PORITSKY, *J. appl. Mech., Trans A.S.M.E.* **72**, 191–201 (1950).
[18] B. S. CAIN, Discussion of Ref. [3]. *J. appl. Mech., Trans A.S.M.E.* **72**, 465–466 (1950).
[19] K. L. JOHNSON, *J. appl. Mech.* **25**, 339–346 (1958).
[20] K. L. JOHNSON, *J. appl. Mech.* **25**, 332–338 (1958).
[21] A. D. DE PATER, On reciprocal pressure between two elastic bodies. *Proc. Symposium on Rolling Contact Phenomena*, pp. 29–74. Elsevier, Amsterdam (1962).
[22] J. J. KALKER, *The Transmission of Force and Couple Between Two Elastically Rolling Spheres*. To be published.
[23] D. J. HAINES and E. OLLERTON, *Proc. Instn mech. Engrs*, **177**, 95–114 (1963).
[24] P. J. VERMEULEN and K. L. JOHNSON, *J. appl. Mech.* **31**, 338–340 (1964).
[25] S. P. TIMOSHENKO and J. N. GOODIER, *Theory of Elasticity*, 2nd edition, p. 379. McGraw-Hill, New York (1951).

(*Received* 23 *October* 1964)

Zusammenfassung—Die dynamische Instabilität der Drehgestelle und Radsätze wird durch die zwischen den Rädern und Schienen zur Auswirkung kommenden Nachwirkkräfte in Zusammenwirkung mit der Radkonizität verursacht. In diesem Beitrag wird der wichtige Fall einer Instabilität untersucht, wo die Räder mehr profiliert als konisch gestaltet sind. Es werden Bewegungsgleichungen formuliert und Stabilitätskriterien angegeben, welche darauf hin deuten, welche Effekte auftreten, wenn die verschiedenen Parameter des Systems verändert werden. Ausserdem wird die Art der Bewegung bei kritischer Geschwindigkeit untersucht und die Art der durch die vorwärts gerichtete Fahrzeugbewegung und die seitlich gerichtete Bewegung des Drehgestelles oder Radsatzes verursachten Energiewandlung erklärt.

Абстракт—Динамическая неустойчивость железнодорожных тележек и комплектов колес имеет причиной комбинированное действие конической формы колес и сил скольжения между колесами и рельсами. В данной бумаге исследуется неустойчивость в важном случае, где колеса имеют профиль вместо простой конической формы. Формулируются уравнения движения и дается критерий устойчивости, который указывает на воздействие изменения различных параметров системы.

Исследуется природа движения при критической скорости и обьясняется вид превращения энергии между поступательным движением экипажа и боковым движением тележки или комплекта колес.